Research Article | Vol. 26, No. 8 | 16 Apr 2018 | OPTICS EXPRESS 10527
Optics EXPRESS

Coherent anti-Stokes Raman scattering as an effective tool for visualization of single-wall carbon nanotubes

ALESIA PADDUBSKAYA,[1,2,*] ANDREJ DEMENTJEV,[2] ANDRIUS DEVIŽIS,[2] RENATA KARPICZ,[2] SERGEY MAKSIMENKO,[1] AND GINTARAS VALUŠIS[2]

[1]*Research Institute for Nuclear Problems, Belarusian State University, Bobruiskaya str. 11, Minsk, 220030, Belarus*

[2]*Center for Physical Sciences and Technology, Saulėtekio ave. 3, Vilnius, LT-10257, Lithuania*

[*]*paddubskaya@gmail.com*

Abstract: Strong vibrational coherent anti-Stokes Raman scattering (CARS) signal was observed in single-wall carbon nanotubes (SWCNTs) having three different average diameters (about 0.8 nm, 1.1 nm and 1.3 nm) under optical excitation close to electronic resonance energies of nanotubes. By varying the excitation power from 1 up to 200 μW an optimal regime for non-destructive investigation of nonlinear properties of SWCNTs was determined. The possibility to detect a strong coherent nonlinear signal from small SWCNT-bundles together with CARS advantages over Raman scattering, such as high imaging rate, open new opportunities for fast three-dimensional visualisation of SWCNTs in a polymer matrix.

OCIS codes: (190.4380) Nonlinear optics, four-wave mixing; (300.6230) Spectroscopy, coherent anti-Stokes Raman scattering;(160.4236) Nanomaterials; (100,6890) Three-dimensional image processing.

References and links

1. P. J. F. Harris, *Carbon Nanotube Science: Synthesis, Properties and Applications* (Cambridge University, 2009).
2. S. Abdalla, F. Al-Marzouki, A. A. Al-Ghamdi, and A. Abdel-Daiem, "Different technical applications of carbon nanotubes," Nanoscale Res. Lett. **10**, 358–368 (2015).
3. S. H. Yoshimura, S. Khan, H. Maruyama, Y. Nakayama, and K. Takeyasu, "Fluorescence labeling of carbon nanotubes and visualization of a nanotube-protein hybrid under fluorescence microscope," Biomacromolecules **12**, 1200–1204 (2011).
4. J. Loos, A. Alexeev, N. Grossiord, C. E. Koning, and O. Regev," Visualization of single-wall carbon nanotube (swnt) networks in conductive polystyrene nanocomposites by charge contrast imaging," Ultramicroscopy **104**, 160–167 (2005).
5. M. IIcikova, M. Danko, M. Doroshenko, A. Best, M. Mrlik, K. Csomorova, M. Slouf, D. Chorvat Jr., K. Koynov, and J. Mosnacek, "Visualization of carbon nanotubes dispersion in composite by using confocal laser scanning microscopy," Eur. Polym. J. **79**, 187–197 (2016).
6. Z. Li, J. Ding, P. Finnie, J. Lefebvre, F. Cheng, C. T. Kingston, and P. R. L. Malenfant, "Raman microscopy mapping for the purity assessment of chirality enriched carbon nanotube networks in thin-film transistors," Nano Res. **79**, 2179–2187 (2015).
7. C. Thomsen, S. Reich, and J. Maultzsch, "Resonant raman spectroscopy of nanotubes," Phil. Trans. R. Soc. Lond. A **362**, 2337–2359 (2004).
8. A. Jorio, A. G. Souza Filho, G. Dresselhaus, M. S. Dresselhaus, R. Saito, J. H. Hafner, C. M. Lieber, F. M. Matinaga, M. S. S. Dantas, and M. A. Pimenta, "Joint density of electronic states for one isolated single-wall carbon nanotube studied by resonant raman scattering," Phys. Rev. B **63**, 245416 (2001).
9. H. Kataura, Y. Kumazawa, Y. Maniwa, I. Umezu, S. Suzuki, Y. Ohtsuka, and Y. Achiba, "Optical properties of single-wall carbon nanotubes," Synth. Met. **103**, 2555 – 2558 (1999).
10. J.-X. Cheng, A. Volkmer, and X. S. Xie, "Theoretical and experimental characterization of coherent anti-stokes raman scattering microscopy," J. Opt. Soc. Am. B **19**, 1363–1375 (2002).
11. Y. Wang, C.-Y. Lin, A. Nikolaenko, V. Raghunathan, and E. O. Potma, "Four-wave mixing microscopy of nanostruc-tures," Adv. Opt. Photon. **3**, 1–52 (2011).
12. H. Kim, T. Sheps, P. G. Collins, and E. O. Potma, "Nonlinear optical imaging of individual carbon nanotubes with four-wave-mixing microscopy," Nano Lett. **9**, 2991–2995 (2009).

#321014 https://doi.org/10.1364/OE.26.010527
Journal © 2018 Received 31 Jan 2018; revised 15 Mar 2018; accepted 16 Mar 2018; published 11 Apr 2018

Optics EXPRESS

13. W. Min, S. Lu, G. R. Holtom, and X. S. Xie, "Triple-resonance coherent anti-stokes raman scattering microspectroscopy," Chem. Phys. Chem. **10**, 344–347 (2009).
14. A. S. Duarte, J. Rehbinder, R. R. B. Correia, T. Buckup, and M. Motzkus, "Mapping impurity of single-walled carbon nanotubes in bulk samples with multiplex coherent anti-stokes raman microscopy," Nano Lett.**13**, 697–702 (2013).
15. T. Sheps, J. Brocious, B. L. Corso, O. T. Gül, D. Whitmore, G. Durkaya, E. O. Potma, and P. G. Collins, "Four-wave mixing microscopy with electronic contrast of individual carbon nanotubes," Phys. Rev. B **86**, 235412 (2012).
16. E. M. Vartiainen, H. A. Rinia, M. Müller, and M. Bonn, "Direct extraction of raman line-shapes from congested cars spectra," Opt. Express **14**, 3622–3630 (2006).
17. A. Hartschuh, E. J. Sánchez, X. S. Xie, and L. Novotny, "High-resolution near-field raman microscopy of single-walled carbon nanotubes," Phys. Rev. Lett. **90**, 095503 (2003).
18. I. Baltog, M. Baibarac, and S. Lefrant, "Coherent anti-stokes raman scattering on single-walled carbon nanotube thin films excited through surface plasmons," Phys. Rev. B **72**, 245402 (2005).
19. M. V. Shuba, A. G. Paddubskaya, P. P. Kuzhir, S. A. Maksimenko, V. K. Ksenevich, G. Niaura, D. Seliuta, I. Kasalynas, and G. Valusis, "Soft cutting of single-wall carbon nanotubes by low temperature ultrasonication in a mixture of sulfuric and nitric acids," Nanotechnology **23**, 495714 (2012).
20. A. V. Naumov, O. A. Kuznetsov, A. R. Harutyunyan, A. A. Green, M. C. Hersam, D. E. Resasco, P. N. Nikolaev, and R. B. Weisman, "Quantifying the semiconducting fraction in single-walled carbon nanotube samples through comparative atomic force and photoluminescence microscopies," Nano Lett. **9**, 3203–3208 (2009).
21. A. Dementjev, V. Gulbinas, A. Serbenta, M. Kaucikas, and G. Niaura, "Coherent anti-stokes raman scattering spectroscope/microscope based on a widely tunable laser source," J. Mod. Opt. **57**, 503–509 (2010).
22. A. Dementiev, G. Mordas, V. Ulevicius, and V. Gulbinas, "Investigation of microstructured chitosans by coherent anti-stokes raman microscopy," J. Microsc. **257**, 217–225 (2015).
23. J.-X. Cheng, A. Volkmer, L. D. Book, and X. S. Xie, "An epi-detected coherent anti-stokes raman scattering (e-cars) microscope with high spectral resolution and high sensitivity," J. Phys. Chem. B **105**, 1277–1280 (2001).
24. C. Stanciu, R. Ehlich, V. Petrov, O. Steinkellner, J. Herrmann, I. V. Hertel, G. Y. Slepyan, A. A. Khrutchinski, S. A. Maksimenko, F. Rotermund, E. E. B. Campbell, and F. Rohmund, "Experimental and theoretical study of third-order harmonic generation in carbon nanotubes," Appl. Phys. Lett. **81**, 4064–4066 (2002).

1. Introduction

A unique quasi-one-dimensional structure of single-wall carbon nanotubes (SWCNTs) specifies their unusual physical properties and, correspondingly, advanced properties of CNT-based materials in many practical applications [1,2]. Among them, there are a lot of applications where visualization of individual CNTs or CNT-based networks is required [3–6]. However, due to a high aspect ration and small diameter, direct observation and volume distribution control of individual CNTs in a composite material, for example in polymer matrix, is a challenging task. Various techniques have been developed for SWCNTs characterization. In particular, optical methods have been found to be not only powerful instruments to investigate their structural and electronic properties, but also they serve as a tool for visualization of SWCNTs. One of the mechanism actually used for CNTs imaging is the vibrational contrast in spontaneous Raman scattering. To date, the properties of Raman spectra of carbon nanotubes have been described in detail, for example in [7]. In particular, it has been shown that the enhanced optical response is observed when the energy of excitation light resonates with electronic transitions in a nanotube [8]. Therewith, the electronic structure of individual SWCNTs is rather well-known [9].

In spite of the fact that resonance Raman spectroscopy is well developed and widely used, there are some specific disadvantages inherent in this method. As a rule, a long acquisition time and high laser power is required in applying to image SWCNTs in biological samples, polymer matrices, etc. [3,4]. All these obstacles can be successfully circumvented using nonlinear optical techniques [10].

Due to high sensitivity, chemical selectivity, spatial resolution and high signal-to-noise ratio the coherent anti-Stokes Raman scattering (CARS) has received priority attention in the family of nonlinear techniques for investigation and visualization of different nanoparticles [11]. By analogy with the spontaneous Raman scattering technique, the enhancement of anti-Stokes signal in CARS is expected if exciting light overlaps with energies of electronic transitions in nanotubes. It is worth noting that in comparison with the resonance Raman technique, where high average power is necessary to reach the effect due to the process low cross-section, the CARS technique

Optics EXPRESS

has a preference allowing detection of individual nanoparticles with the relatively low average excitation power [10, 12]. This is related to the fact that the CARS is a four-wave mixing process, where multi-resonance processes provide a strong enhancement of scattering efficiency. Wei Min et al. [13] have shown that the triple-resonance condition can be satisfied by tuning the spectral range of CARS microspectroscope allowing thus the sensitivity of normal CARS enhancement by 10^3 to 10^5 times. A better spatial contrast of impurity maps (the plot of the ratio between G- and D- bands) has also been demonstrated in [14] by investigation of the local defects in a non-purified spin-coated SWCNTs.

Despite that there are disadvantage in CARS technique related to its technical specifications, in particular, the response strongly depends on matching of the setup configuration and intrinsic optical properties of the investigated materials. The sensitivity to the wavelength of exciting light has clearly been demonstrated in [15]. Another inconvenience of the coherent Raman scattering technique is related to the presence of a non-resonance contribution that leads to a complex shape of CARS spectra and thus can induce the reduction in the vibrational contrast [10, 16]. Moreover, the spatial resolution of "classical" CARS technique is not capable to visualize individual SWCNTs. However, other techniques proposed to improve spatial resolution, like surface enhanced scattering (SERs), also are not suitable for large scale 3D visualization [17, 18] due to extreme sensitivity to sample thickness. In this case, the resonance enhancement can be the way to improve the sensitivity and therefore to reduce the detection threshold of CNTs embedded in an organic matrix. It is worth noting that these aspects of application of CARS technique have not been considered for CNTs in details as yet.

In this article, we specify the experimental conditions – via variation of CNTs diameter and excitation power – to register strong CARS response from individual SWCNTs or small bundles, and demonstrate the potential of such a technique for 3D visualisation of the spatial distribution of SWCNTs, for example, in a polymer matrix.

2. Materials and method

Three types of commercially available purified SWCNTs with different diameters were used in our experiments: electric-arc-produced SWCNT bundles (CarboLex, Inc) obtained using nickel-yttrium catalyst, with SWCNT diameters from 1.2 to 1.5 nm and purity between 50 % and 70 %, and SWCNT bundles (Nano-C, Inc) produced by gas-phase catalysis (HiPCO process), with average SWCNT diameter 1.1 nm and purity exceeding 95 %, and SWCNTs (SWeNT, Inc., SG65i purchased from Sigma-Aldrich) produced by chemical vapor deposition on a cobalt-molybdenum catalyst, with an average SWCNT diameter of 0.7 - 0.9 nm and purity exceeding 95 %. More details of CNTs characterization can be found in [19] and [20]

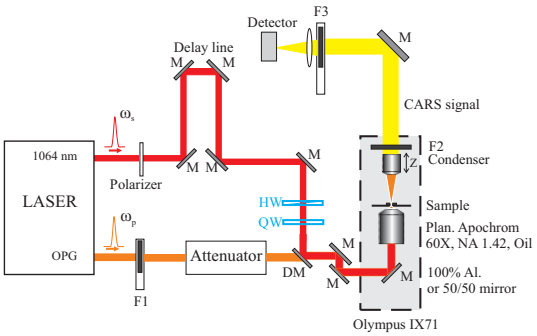

Fig. 1. Optical scheme of the CARS microscope: F1 and F2 denotes revolvers with filters; M labels mirror; DM is dichroic mirror; HW shows half-wave plate; QW is quarter-wave plate; dashed grey area denotes inverted microscope with oil-immersion objective.

Optics EXPRESS

Optical properties of CNTs were measured using home-made CARS microscope (see [21] and [22] for more details of the experimental setup) based on compact laser source (EKSPLA Ltd.). The schematic setup is presented in Fig. 1. The picosecond (6 ps) laser consisted frequency doubled Nd:YVO_4 pump laser with the pulse repetition rate of 1 MHz and equipped with a travelling wave optical parametric generator (OPG) which allowed continuous wavelenght tuning from 695 to 2300 nm. The pulse duration as small as several ps was a reasonable compromise between high pulse intensity and narrow (1-3 cm^{-1}) spectral bandwidth [23]. The radiation after OPG was used as the pump excitation beam for CARS signal generation while the fundamental laser mode (1064 nm) served as the Stokes excitation beam. A spatial filter was used to improve the beam profile before directing it into the microscope. The temporal overlap of two excitation beams was controlled by a delay line. All measurements were done at zero delay time between the pump and Stokes pulses with parallel polarization. The beams were introduced collinearly to an inverted microscope (Olympus IX71) with oil-immersion objective (Olympus, Plan Apochrom., 60×, NA 1.42). The objective with high NA allowed us to focus the excitation light into a spot size around 450 nm in diameter, giving a power density of 50 GW/cm^2 for incoming 1 mW power. The measurements were done in the forward detection scheme. The CARS signal in the range from 845 nm up to 782 nm was collected by objective with NA 0.4 and detected with the avalanche photodiode (SPCM-AQRH-14, Perkin Elmer) connected to a multifunctional board PCI 7833R (National Instruments Ltd). Long-pass and short-pass filters were used as a blocking tools for spectral separation of the CARS signal. The possibility to control individually the power level of pump and Stokes beams allowed us to do direct measurement of CARS signal amplitude versus beam energy. To account for the spectral dependence of the OPG generator efficiency, the CARS signal intensity was normalized to the power of the OPG radiation. The spectra were recorded with a typical detection rate of 5 cm^{-1} per second.

A piezoelectric scanning system (Physik Instrumente GmbH & Co.) was used for two-dimensional scanning of sample. To obtain 3D images of polymer/CNTs composites the microscope focus was displaced in 1 μm steps in vertical direction (along Z -axis). Two-dimensional X-Y scanning was repeated for each step to give a slice. The 3D images were reconstructed by stacking all slices (in average 20 slices per image) using free software package ImageJ.

Samples for spectral measurements were prepared by depositing CNT-powder on the surface of microscopic cover glass. Commercially available polyvinyl alcohol (PVA, Sigma-Aldrich) was used as polymeric matrix for production of the composite materials containing SWCNTs. Briefly, initial CNTs (SWCNT with average diameter 1.1 nm was used in this part of work) were dispersed for 1 hour in 1% aqueous SDS solution using the tip ultrasound (UZDN-T, Russia, 44 kHz). In order to remove bundles and residue catalic metal particles after ulrasonication the suspension was centrifuged at 15,000g for 3 h (Elmi CM-50). To avoid sample "overheating", 10 min pauses were made after every 10 min centrifuging. The supernatant was collected and mixed with PVA /water suspension (30 mg/ml). The resulting mixture was poured between two microscope cover glasses and dried at room temperature. To deduce the applicability of nonlinear technique for 3D visualization of CNTs in composites with different CNT fractions, the initial suspension was diluted 5 and 10 times, and corresponding 3D images were investigated.

3. Results and discussions

The CARS spectra at different pump power for the samples with SWCNTs of three different diameters are presented in Figs. 2(a)-2(c). The entire spectral range can be divided into two different parts: from 1200 cm^{-1} up to 1500 cm^{-1} and from 1500 cm^{-1} up to 1700 cm^{-1}. The response in the first range may be attributed to non-resonance contribution, while the response in the second part is conditioned by resonant process. A large Raman-like response was obtained from samples having small fractions of 0.8 and 1.1 nm diameter CNTs, whereas

Optics EXPRESS

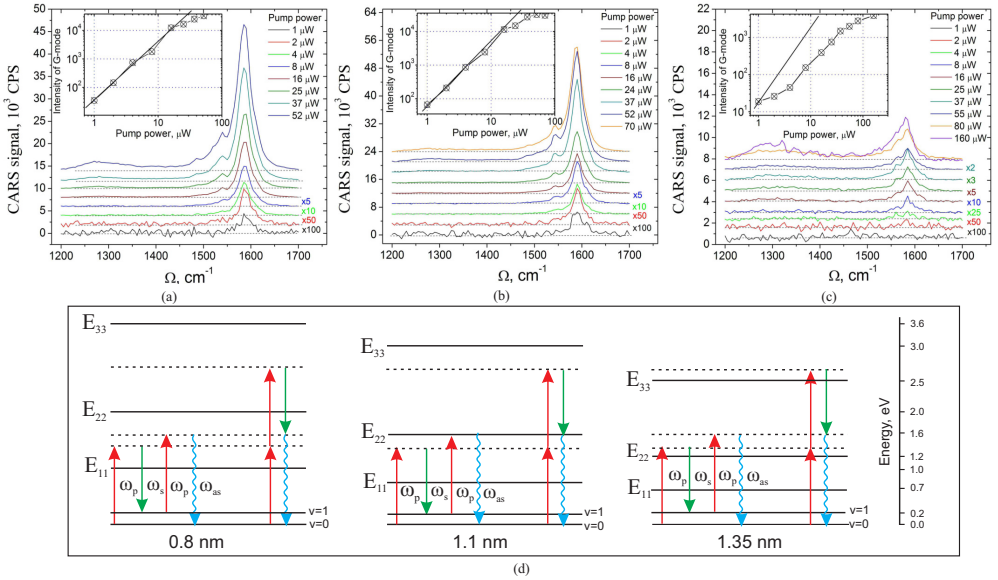

Fig. 2. CARS spectra of SWCNTs measured at different pump power: (a) 0.8 nm, (b) 1.1 nm, (c) 1.35nm. All spectra were obtained with 10 μW Stokes average power and at zero time delay between the pump and Stokes pulse. Insets: variation of G-band intensity as a function of the pump power. (d) Schematic diagram of energy levels for s-SWCNTs at different diameters (from [9]).

the sample with 1.35 nm diameter CNTs revealed essentially reduced response even for higher concentration of nanotubes. By analogy with the linear optical properties, such a difference in the nonlinear response can be related to the CNT diameter. Figure 2(d) shows the energy level diagrams for SWCNTs with different average diameters. The vertical arrows indicate the pump(red)/Stokes(green)/anti-Stokes(blue) photons involved in the excitations. The energy difference between pump and Stokes photons corresponds to the G-mode energy (1590 cm^{-1}). As follows from Figs. 2(a) and 2(b), the relative intensity of non-resonant background for 1.1 nm CNTs is smaller than that for 0.8 nm CNTs. Such a difference can be easily understood by taking into account the following facts: in the case of 1.1 nm CNTs the pump and anti-Stokes photons are in resonance with E_{22} energy level giving rise, along with the resonance due to the energy difference between pump and Stokes photons, to a triple resonance. It leads to the enhancement of CARS signal in resonance range (G-mode) and, as the result, reduces relative contribution of non-resonance background.

One can note that similar Raman-like CARS spectra of SWCNTs were presented in [14], where such a large signal was associated with the spontaneous Raman contribution from pump beam. In order to estimate Raman contribution to the total CARS signal in our experiments, independent spectra obtained by consecutively blocking the Stokes and the pump beam were also measured. It was found that the pump and the Stokes beams measured independently contribute negligibly to the total signal.

As mentioned earlier, the spectra of CNTs with large diameter (1.35 nm) exhibit dramatic change, Fig. 2(c). First of all, the CARS-response turned out to be rather weak. In order to obtain the traceable signal from there SWCNTs, a material with bigger fraction of CNTs has been chosen, but even then, the total response was approximately 8 times weaker as compared with 0.8 nm or 1.1 nm CNTs. As follows from the energy diagram (see Fig. 2(d)), such a behavior can be explained by the enhancement of two-photon absorption due to resonance with E_{33}. As

Optics EXPRESS

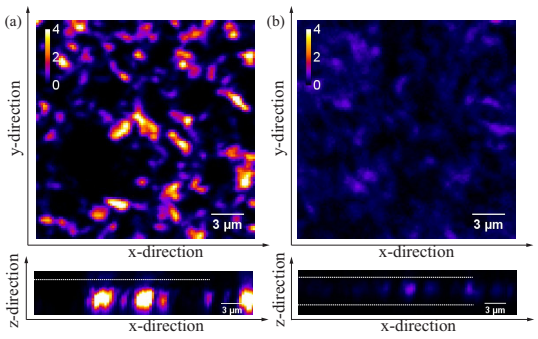

Fig. 3. CARS images (XY and XZ) of SWCNT distributions on a cover glass: (a) SWCNTs with 1.1 nm and (b) SWCNTs with 1.3 nm diameters. The image size is 20 μm×20 μm. The pump and Stokes beam powers were 20 μW. For the CARS images, ω_p-ω_s was tuned to G-band (1585 cm^{-1}). The pixel dwell time was 20 ms. The interface air/CNTs and glass/CNTs are indicated by horizontal white lines (only for XZ images). All spectra were normalized to a maximal signal value obtained for SWCNTs with 1.3 nm diameters. The imaging contrast is 1:1000.

a result, contribution of the non-resonance part increases. From imaging point of view, such a difference in CARS-response of CNTs dramatically decreases the sensitivity of CARS technique for spatial visualization of CNTs having large diameter. To demonstrate the interdependence between the settings of experimental setup and CNTs properties, the CARS images of small agglomerates of SWCNTs with 1.1 and 1.35 nm diameter are presented on Fig. 3. All images were normalized to a maximal signal value obtained for small agglomerates of SWCNTs with 1.3 nm diameter. Note that the intensity changes four order of magnitude when the system is tuned between on-resonance and off-resonance. However, the presence of nonresonance background complicates the interpretation of the results.

The dependencies of the G-band intensity on the pump power are presented in the inserts of Figs. 2(a)- 2(c). It should be noted that in accordance with the CARS theory (for example see [10]) we have $I_{CARS} \propto I^2_{pump} I_{Stokes}$. Therefore, at 0.8 nm and 1.1 nm SWCNTs the amplitude of the G-band grows quadratically up to 20 μW of the pump power, when the Stokes power is kept fixed at 10 μW. Further increase in the pump power leads to the saturation of the G-band amplitude. It means that new energy relaxation channel that does not contribute the CARS signal has opened. One of the possible channel of the energy relaxation can be a fluorescence caused by an increase of the two-photon absorption at higher powers. Phenomenologically the revealed strong nonlinearity of the light interaction with carbon nanotubes indicates the violation of a power expansion of the medium polarization allowing introducing the power-independent nonlinear susceptibility $\chi^{(3)}$ [24]. Our experiment clearly demonstrates that the saturation power does not depend on agglomerate sizes and is mainly determined by light intensity on the sample surface.

From this we conclude that our experiments reveal a large CARS response due to electronic resonance in CNTs of any diameters. Actually, the larger signal was obtained with CNTs of 0.8 and 1.1 nm diameter. In this case, the electron transition energy appears to be close to energy of exciting pump photon, and therefore the pre-resonance regime is realized. When the energy of pump photon is tuned to electronic transition energy, enhancement of the two-photon absorption occurs. It affects the amplitude of resonance band and, in general, reduces CARS response. Furthermore, for 0.8 nm and 1.1 nm CNTs, the quadratic dependence of the G-band saturates at pump power ~ 20 μW (10 ps, 1MHz) which corresponds to ~ 1 GW/cm^2 peak intensity. For 1.35 nm CNTs the saturation was obtained at ~ 0.3 GW/cm^2 peak intensity.

The strong vibrational CARS signal, in comparison with the electronic contribution obtained

Optics EXPRESS

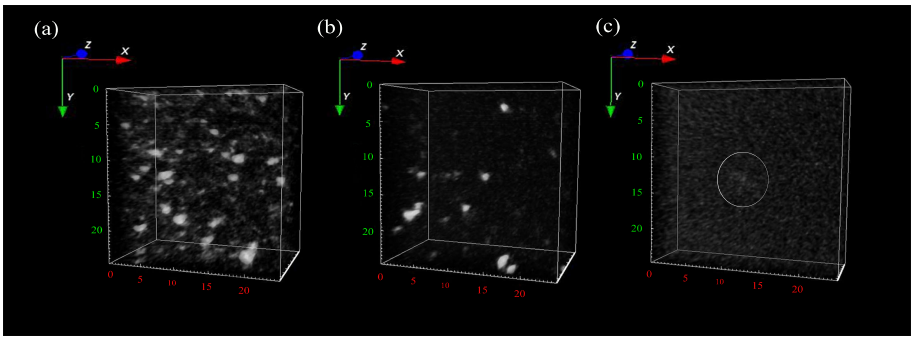

Fig. 4. The volume images of PVA/SWCNT composites: (a) initial concentration, (b) diluted 5 times, (c) diluted 10 times; the circle indicates a single luminescent spot. All images were obtained with 50 μW Stokes average power and 80 μW pump average power. Pixel dwell time was 20 ms.

for CNTs of small diameter, allows us to visualize a distribution of this kind of CNTs embedded in the polymer (PVA) matrix (Fig. 4). The CARS spectra taken from different points of one of XY slice are presented in Fig. 5. One can observe that according to our preparation technique the CNTs are homogeneously distributed over the polymer matrix. Furthermore, in spite of the fact that large spots can be attributed to CNTs agglomerates, small bright spots in Fig. 4(a) have the characteristic CARS spectra with discernible G-band (the curve corresponding to point 3 in Fig. 5) and can be attributed to small bundles of CNTs. It should be noted that the pure matrix does not produce registerable CARS response at excitation energies of several μW.

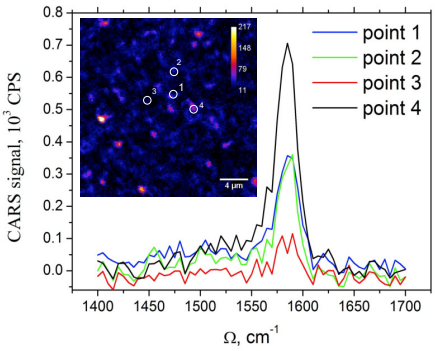

Fig. 5. CARS spectra of SWCNTs in PVA matrix measured at different points. The CARS image of PVA composite with embedded CNTs is depicted in the insert. The image size is 25 μm×25 μm. The pump and Stokes beam powers were 50 μW. ω_p-ω_s was tuned to G-band (1585 cm^{-1}). The pixel dwell time was 50 ms.

Images presented in Figs. 4(b) and 4(c) correspond to samples diluted 5 and 10 times, respectively, as compared with the sample with initial concentration, Fig. 4(a). As one can see, a number of bright spots in pictures decrease proportionally, so that a single spot (indicated by circle) in the case of 10 times decreased concentration of CNTs was detected. The gray background in Fig. 4(c) is due to noise of the avalanche diode.

Optics EXPRESS

4. Conclusions

The obtained results demonstrate the effective visualization method of CNTs using the CARS non-linear optical technique. We have found that effective application of this technique requires coherency of the photons of light source of CARS microscope with the energies of optical transitions (Kataura plot) of CNTs. Large well-registrable CARS signal has been obtained at μW-range excitation in CNTs with 0.8 nm and 1.1 nm diameters, when the contribution from two-photon process is relatively small. Energy threshold is about 18 μW behind which the quadratic dependence of the G-mode intensity on pump power is violated. The effect can be attributed to new energy relaxation channel due to fluorescence caused by increase of the two-photon absorption at higher powers. The ability to detect strong coherent nonlinear signal from small SWCNT-bundles, along with a high imaging rate inherent to CARS technique, allows us to propose the coherent anti-Stokes Raman scattering as a new fast and effective tool for 3D visualization of single-walled carbon nanotubes and the control of their spatial distribution, for example, in a polymer matrix or in biological samples, non-label visualization method of cells or organelles.

Funding

Research Council of Lithuania Foundation (S-LU-18-6).